

Cultivation of *Chlorella vulgaris* in anaerobically digested gelatin industry wastewater

G. C. Blanco, M. J. Stablein and G. Tommaso

ABSTRACT

This work aimed to study the effect of using anaerobically digested gelatin industry wastewater as a culture medium for the cultivation of *Chlorella vulgaris* microalgae in bubble column photobioreactors (PBRs). Batch experiments were carried out to determine the growth kinetics by inoculating microalgae in wastewater prepared with different dilutions and supplemented with Bold's Basal Medium (BBM). From the values of the saturation constants ($K_S = 50.25 \text{ mgN-NH}_4^+ \cdot \text{L}^{-1}$) and substrate inhibition ($K_I = 28.12 \text{ mgN-NH}_4^+ \cdot \text{L}^{-1}$) obtained in the adjustment to the Andrews kinetic model ($R^2 = 0.817$), the PBRs achieved specific maximum growth rates (μ_{\max}) of 0.343 d^{-1} , biomass productivity of $0.141 \text{ g} \cdot \text{L}^{-1} \cdot \text{d}^{-1}$, lipid content of 12.45%, lipid productivity of $17.63 \text{ mg} \cdot \text{L}^{-1} \cdot \text{d}^{-1}$ and instantaneous ammoniacal nitrogen consumption rates of 20.06 and $14.22 \text{ mg} \cdot \text{L}^{-1} \cdot \text{d}^{-1}$. The addition of wastewater to the culture medium provided an increase in biomass productivity of 57.45% in relation to the negative control. The results obtained demonstrate the high efficiency of *C. vulgaris* in the removal of nitrogenous compounds and the potential of using anaerobically digested gelatin industry wastewater in the production of microalgae biomass.

Key words | biomass production, *Chlorella vulgaris*, gelatin industry, kinetic modelling, lipids, wastewater post-treatment

G. C. Blanco

G. Tommaso (corresponding author)

Laboratory of Environmental Biotechnology,

Department of Food Engineering,

University of São Paulo,

225, Duque de Caxias Norte, Pirassununga, São

Paulo 13635-900,

Brazil

E-mail: tommaso@usp.br

M. J. Stablein

Department of Agricultural and Biological

Engineering,

University of Illinois at Urbana-Champaign,

1304 W Pennsylvania Avenue, Urbana, IL 61801,

USA

HIGHLIGHTS

- The use of wastewater in bubble column photobioreactors (PBRs) provided a 57.45% increase in biomass productivity (PB).
- Andrews model successfully predicted the growth kinetics of *C. vulgaris* in wastewater ($R^2 = 0.817$).
- Ammoniacal nitrogen (N-NH_x) was preferred compared with nitrate (N-NO_3) during the operation of photobioreactors.
- The first-order decay model with residual successfully predicted the kinetics of nitrate (N-NO_3) consumption.
- Two first-order decay models with residuals in series better represented the ammoniacal nitrogen (N-NH_x) depletion.

INTRODUCTION

Contamination of water bodies from consumption of natural resources and unsustainable practices is of increasing importance. Advanced wastewater treatment processes that can

simultaneously replenish these resources and minimize environmental contamination are essential to our society. Conventional anaerobic methods aimed at removing carbonaceous material are not effective in removing nutrients, therefore, there is a need in many cases to install post-treatment units (Mai *et al.* 2018). In this context, the cultivation of microalgae has been shown to be an alternative to tertiary treatment, since, in

This is an Open Access article distributed under the terms of the Creative Commons Attribution Licence (CC BY 4.0), which permits copying, adaptation and redistribution, provided the original work is properly cited (<http://creativecommons.org/licenses/by/4.0/>).

doi: 10.2166/ws.2020.263

addition to the ability to absorb potentially toxic nutrients and metals present in aquatic environments, they accumulate lipids, produce oxygen, and capture the carbon dioxide present in the atmosphere. The yields of these products vary according to the species and can be induced by system disturbances, resulting in cellular stress, as well as through the adaptation of certain cultivation strategies (Tan & Lee 2016).

Despite the low nitrogen content in the composition of microalgal biomass, ranging between 1% and 10%, this element is essential in the regulation of metabolic pathways and is the most critical nutrient for the growth of microalgae after carbon (Pistorius *et al.* 1978). Some algae assimilate inorganic nitrogen in different forms such as nitrate (N-NO_3^-), nitrite (N-NO_2^-), and ammoniacal nitrogen (N-NH_x). During the assimilation process, the inorganic nitrogen compounds pass through the cytoplasmic membrane where enzymatic reductions occur to form ammonium (N-NH_4^+), which is later converted to organic compounds, such as the necessary peptides, amino acids, proteins, enzymes, and nucleic acids for the growth of biomass (Li *et al.* 2019).

The assimilation of ammoniacal nitrogen requires less energy, and it is the preferred nitrogen source of microalgae (Maestrini *et al.* 1986). According to Li *et al.* (2019), if ammoniacal nitrogen, nitrate, or nitrite are present in the culture medium, the microalgae will consume ammoniacal nitrogen first, then nitrite, and finally nitrate. However, the excess of ammoniacal nitrogen in the culture medium presents negative aspects such as volatilization and the inhibition of microbial growth, and thus, nitrate becomes the most used form for the cultivation of microalgae, as it is chemically stable in aquatic environments (Florencio & Vega 1983).

Several studies have cultivated microalgae using anaerobically treated wastewater from the food industry; however, few studies have addressed the inhibitory effect of ammoniacal nitrogen and the kinetic modelling of microbial growth based on consumption of nitrogen compounds in bubble column photobioreactors (PBRs) when fed with this type of wastewater. The wastewater produced by the gelatin industry has high loads of proteins, sulphides, and organic nitrogen. Wastewater of this type, when treated by anaerobic reactors, presents wastewater with high concentrations of ammoniacal nitrogen (N-NH_x), and this is due to the degradation of proteins present in the organic material (Ramsay & Pullammanappallil 2001). During the degradation of protein-

rich materials, proteins are hydrolyzed to peptides and subsequently to amino acids that are rapidly fermented by fermentative acidogenic bacteria and converted into short-chain volatile acids, carbon dioxide, and ammoniacal nitrogen. Each type of wastewater generated in food processing leads to specific considerations for the choice of treatment technology employed (Janosz Rajczyk 1993).

Kinetic models describe the growth of microorganisms and the rate of substrate consumption during operation, providing relevant data for the design of high-efficiency photobioreactors (PBRs). According Eze *et al.* (2018), microalgae growth and the rate of algae biomass accumulation with constant light intensity, temperature, and homogeneous mixing is typically determined by substrate and nutrient availability. Thus, a robust kinetic model is essential to predict substrate consumption, cell growth, and optimize operating conditions for the cultivation of microalgae in wastewater. Several mathematical models have been adjusted to try to describe the growth of microorganisms in PBRs. The kinetic models normally applied in studies of microalgae specific growth rates (μ), using one of the three main substrates (inorganic carbon, nitrogen, or phosphorus) as functions, are the Monod and Andrews models (Chojnacka & Marquez-Rocha 2004). Generally, the growth rates of microorganisms (μ) in the Monod models are limited by the substrate availability, whereas the Andrews model growth rates are limited by the excess of substrate in the culture medium that inhibits cell growth (Eze *et al.* 2018). Therefore, the concentration of nutrients can determine the maximum specific growth rate of microalgae (μ_{max}). In this sense, this work seeks to evaluate the viability of cultivating microalgae species *Chlorella vulgaris* in anaerobically digested gelatin industry wastewater in order to determine the kinetic parameters of microbial growth and substrate consumption, the biomass productivity, the efficiency of the removal of nitrogen compounds (N-NH_x and N-NO_3^-), and the lipid productivity.

METHODS

Inoculum

The inoculum of the microalgae *Chlorella vulgaris* clone BMAK D1 was provided by the Microalgae Engineering

Laboratory of the University of São Paulo of Lorena School of Engineering (EEL/USP). The culture was maintained and propagated under aseptic conditions using 250 mL conical flasks in the Environmental Biotechnology Laboratory of the University of São Paulo of Animal Sciences (FZEA/USP) culture collection in modified Bold's Basal Medium (BBM). The inoculum was kept under controlled temperature ($26 \pm 2^\circ\text{C}$) and photoperiod (24/0 hours, light/dark) conditions with an estimated light intensity of 4,600 lumens per square metre (lm/m^2) (Zorn et al. 2017).

Anaerobically digested gelatin industry wastewater

The wastewater used in this work came from the UASB (Upflow Anaerobic Sludge Blanket) reactor of the Gelita Brasil Ltda industry located in Mococa, SP. The collection took place in July 2019 and was performed in triplicate. The collected wastewater was stored in 5.0 L gallons and frozen. Analysis of crude and filtered COD, total Kjeldahl nitrogen (N-NTK), ammoniacal nitrogen (N-NH_x), nitrite (N-NO_2^-), nitrate (N-NO_3^+), organic nitrogen (N-N_{org}), total nitrogen (N-N_T), total phosphorus (P_T), and sulphates (SO_4^{2-}) were performed according to the methods described in *Standard Methods for the Examination of Water and Wastewater* (APHA 1998), while the dissolved oxygen (DO) analysis was performed using a branded probe (SOP model YSI 55). The physicochemical characterization of wastewater was done in triplicate.

In order to control the displacement of the chemical balance of free ammonia (N-NH_3) to ammonium ion (N-NH_4^+) and hydrogen sulphide (H_2S) to hydrogen sulphide (HS^-), the pH of the wastewater was adjusted to 7.5. The adjustment was made by adding aliquots of dilute sulfuric acid (0.05 M) and quantifying the pH values by means of a properly calibrated benchtop digital pH meter (Tecnal model TEC-03MP). In order to prevent light from being blocked due to the high solids concentration and turbidity of the wastewater, the effluent was filtered through a filter system composed of a Kitasato flask and a Büchner funnel with $0.45\ \mu\text{m}$ filter membrane (Unifil ETQ) before the inoculation.

After filtration of the wastewater, the sterilization was carried out by adding $1.0\ \text{mL}\cdot\text{L}^{-1}$ of sodium hypochlorite (5%). The solution was manually homogenized with a glass rod and allowed to stand for 12 hours for complete

elimination of microorganisms (species control). A higher concentration of sodium hypochlorite than conventional sterilization methods was used to promote irreversible oxidation of sulphides. After this period, an indicator test was performed to verify the absence of chlorine in the solution. In cases where residual chlorine was observed, the solution was neutralized with sodium thiosulfate in order to prevent possible interference in the growth of microalgae.

Finally, the wastewater was supplemented with modified Bold's Basal Medium (BBM) to optimize the growth of microorganisms and to supply the nutritional deficiencies of the effluent. Table 1 presents the physicochemical characterization of the anaerobically digested gelatin industry wastewater and the composition of the basal medium used in the supplementation. The wastewater physicochemical parameters were determined experimentally and are presented as averages with Standard Deviation (SD), while the modified BBM is presented with standard composition values.

Calibration curve

The microalgae growth was monitored based on a calibration curve ($R^2 = 0.9996$) designed to convert the

Table 1 | Physicochemical characterization of the wastewater collected in the UASB reactor from the gelatin industry and theoretical composition of the modified Bold's Basal Medium (BBM)

Parameters of modified Bold's Basal Medium	Composition ($\text{mg}\cdot\text{L}^{-1}$)	Parameters of wastewater	Composition ($\text{mg}\cdot\text{L}^{-1}$)
NaNO_3	750	$\text{DQO}_{\text{Crude}}$	170.65 ± 3.61
K_2HPO_4	75	$\text{DQO}_{\text{Filtered}}$	122.20 ± 5.66
KH_2PO_4	175	OD	0.18 ± 0.05
NaHCO_3	75	N-NTK	359.98 ± 1.81
$\text{CaCl}_2\cdot 2\text{H}_2\text{O}$	5	N-NH_4^+	281.90 ± 3.11
$\text{Mg}\cdot\text{SO}_4\cdot 7\text{H}_2\text{O}$	20	N-NO_3^-	0.22 ± 0.01
EDTA	50	N-NO_2^-	10.44 ± 0.30
$\text{FeCl}_3\cdot 6\text{H}_2\text{O}$	4	N- N_T	370.64 ± 2.13
H_3BO_3	4	N- N_{ORG}	78.08 ± 4.92
$\text{ZnSO}_4\cdot 7\text{H}_2\text{O}$	1.5	P_T	2.05 ± 0.06
$\text{Cl}_2\text{Mn}\cdot 7\text{H}_2\text{O}$	0.24	SO_4^{2-}	521.91 ± 14.96
$\text{CuSO}_4\cdot 5\text{H}_2\text{O}$	0.24	pH	7.75 ± 0.07
$\text{CoCl}_2\cdot 6\text{H}_2\text{O}$	0.06		
Na_2MoO_4	0.20		

absorbance (abs) results to biomass concentration ($\text{g}\cdot\text{L}^{-1}$). The wavelength used in quartz cuvette absorbance readings was 680 nm (Guimarães *et al.* 2019), determined using a HACH model DR 2800 spectrophotometer. The curve was generated by operating the batch column photobioreactor with modified Bold's Basal Medium (BBM) (Table 1). When the stationary growth phase was reached, a concentrated aliquot (stock solution) of the reactor was collected and diluted in ten different concentrations, and the absorbance of each curve point was quantified. At the end of the growth period, the remaining volume in the photobioreactor was collected to determine the biomass concentration of the stock solution, relating it to the absorbances obtained in the readings of each dilution. A mathematical relationship was established between the detected signal and the analyte concentration using simple linear regression through which the regression ($a = 0.718$ and $b = -0.0054$) and correlation ($R^2 = 0.9996$) coefficients were obtained. The analysis of errors and accuracy of the standard curve was performed from the Standard Deviation (SD) of each sample data and the Adjusted R-Square (R^2). Plotting of the calibration curve was performed using *Origin 8.0* software.

Inoculum adaptation

Before the kinetic test, the inoculum was adapted to the wastewater. The adaptation process was performed by sequential batches in a 1.0 L bubble column photobioreactor (PBR). The PBR used was fed with increasing concentrations of ammoniacal nitrogen ($C_1 = 7.05 \text{ mg}\cdot\text{L}^{-1}$, $C_2 = 14.09 \text{ mg}\cdot\text{L}^{-1}$, $C_3 = 28.19 \text{ mg}\cdot\text{L}^{-1}$, $C_4 = 56.38 \text{ mg}\cdot\text{L}^{-1}$) and kept in operation until the exponential growth phase and an approximate biomass concentration of $1.2 \text{ g}\cdot\text{L}^{-1}$ in each condition was reached. Then, the batches were discontinued, and the biomass was left for one hour to settle to the bottom of the reactor. After sedimentation of the biomass, 70% of the useful volume (supernatant) of the photobioreactor was removed and refilled with diluted wastewater supplemented with BBM. Once the maximum substrate concentrations tolerated by the inoculum were reached, i.e. the substrate concentration where no inhibition and cell death occurred, the inoculum was collected and recycled to the next stages of the algal adaptation and growth experiment.

Microbial growth kinetics assays

The objective of this assay was to evaluate microalgae growth by monitoring the cumulative biomass production (X) and to determine the optimal substrate concentration (S_{opt}). For the kinetic assay, six different concentrations of ammoniacal (N-NH_x) nitrogen were studied: $C_1 = 7.05 \text{ mgN-NH}_4^+\cdot\text{L}^{-1}$, $C_2 = 14.09 \text{ mgN-NH}_4^+\cdot\text{L}^{-1}$, $C_3 = 28.19 \text{ mgN-NH}_4^+\cdot\text{L}^{-1}$, $C_4 = 56.38 \text{ mgN-NH}_4^+\cdot\text{L}^{-1}$, $C_5 = 112.76 \text{ mgN-NH}_4^+\cdot\text{L}^{-1}$ and $C_6 = 169.14 \text{ mgN-NH}_4^+\cdot\text{L}^{-1}$. Nutrient solutions composed of Bold's Basal Medium (BBM) were prepared as described in Table 1 and added to the reaction flasks to optimize the activity of the microorganisms. Reactor pH was monitored and controlled at 7.5 by the addition of dilute sulfuric acid (0.05 M) to prevent sulphide formation and ammonia nitrogen volatilization due to ammonium ion conversion (N-NH_4^+) to free ammonia (N-NH_3). Finally, three negative reaction flasks were prepared with the same inoculum in Bold's Basal Medium (BBM) without wastewater.

Subsequently, the flasks were incubated in batch at a temperature of 26°C at 200 rpm in a shaker incubator. This equipment was kept in an air-conditioned room and isolated from sunlight. The light used as a power source by microalgae was provided exclusively by 24-hour 6 W LED lamps, resulting in an estimated illuminance of 4,600 lumens per square metre (lm/m^2) (Zorn *et al.* 2017). The microalgae were cultivated without aerators, no CO_2 (carbon dioxide cylinders) feed, and instead, pneumatic agitation was performed. Thus, the only carbon source for the microorganisms was the organic carbon contained in the wastewater, sodium bicarbonate of the basal medium, and the CO_2 present in the atmosphere introduced by the headspace, due to the constant shaking of the bottles (complete mixture). The incubation lasted seven days until biomass production ceased.

Bubble column photobioreactors (PBRs)

The microalgae were grown in a system composed of three batch bubble column photobioreactors with a total volume of 1.2 L each, equipped with external lighting and pneumatic agitation. Bubble column PBRs are characterized by their high volumetric gas transfer coefficients. The bubbling of gases at the bottom of the column provides efficient use of

carbon dioxide and the effective removal of dissolved oxygen. This system provides more efficient operational control over culture conditions and essential growth parameters than open systems, reducing the chance of contamination and the invasion of competing microorganisms. In this type of photobioreactor, the growth of microalgae is normally limited by other variables, such as light intensity and nutrient availability.

Each photobioreactor was composed of a glass column with a 5 mm wall thickness, an internal diameter of 65 mm, a height of 450 mm, and a useful volume of 1.0 L. The aeration system consisted of a diffuser, located at the base of each column, connected by a silicone hose to a diaphragmatic air compressor with a flow rate of 4 L·min⁻¹ for the dispersion of air microbubbles in the system. Figure 1 shows the schematic drawing of the bubble column PBRs used.

Kinetic modelling of microbial growth

The biomass production profiles of each condition were adjusted to the modified Gompertz kinetic model (Equation (1)) described by Mansouri (2017), using *Origin 8.0* software:

$$y = C \times \exp \left\{ -\exp \left[\frac{\mu_{\max} \cdot \exp(1)}{C} \times (\lambda - t) + 1 \right] \right\} \quad (1)$$

In this expression, Y is the concentration of biomass at time t (g·L⁻¹); C is the asymptote of $\ln(X/X_0)$ at time t ; μ_{\max} is the maximum specific growth rate (d⁻¹); λ is the latency phase duration time (d); t is the batch reaction time (d); and \exp is the Euler number.

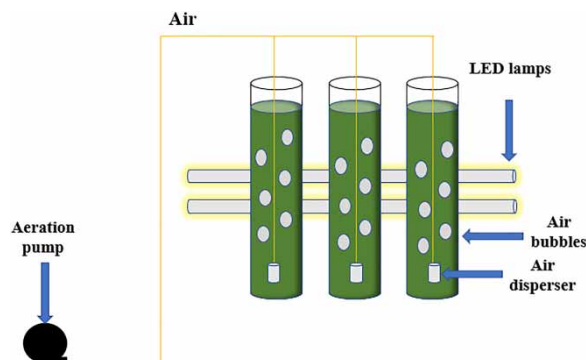


Figure 1 | Schematic drawing of the bubble column photobioreactors (PBRs).

Determining the maximum specific growth rates (μ_{\max}), a graph was constructed that relates the initial substrate concentrations (S) to the maximum specific growth rates (μ_{\max}) of each condition, and the adjustments to known kinetic models were tested by obtaining kinetic parameters and optimal substrate concentration (S_{opt}). As substrate inhibition was observed, the adjusted kinetic model used was the Andrews model (Equation (2)), and the S_{opt} calculated by Equation (3). The adjustment to the Andrews model was performed in the *Origin 8.0* software.

$$\mu = \mu_{\max} \cdot \frac{S}{K_s + S + (S^2/K_i)} \quad (2)$$

$$S_{\text{opt}} = \sqrt{K_s \cdot K_i} \quad (3)$$

In these expressions, μ is the specific growth rate (d⁻¹); K_s is the saturation constant defined by the Monod equation (mgN·NH₄⁺·L⁻¹); K_i is the substrate inhibition constant (mgN·NH₄⁺·L⁻¹); and S_{opt} is the optimal substrate concentration for the operation of bubble column photobioreactors (mgN·NH₄⁺·L⁻¹).

To estimate the parameters of the models, the Levenberg-Marquardt (LM) algorithm was used to adjust the expressions of the equations to the experimental results. The accuracy of the predictive models was investigated using the Adjusted R-Square (R^2) and the Standard Error (SE).

Kinetic modelling of substrate consumption

The consumption of ammoniacal nitrogen (N-NH_x) and nitrate (N-NO₃⁻) were adjusted to the first-order kinetic expression and to the modified first-order kinetic expression, presented in Equation (4) and (5) respectively. Both adjustments were performed using the *Origin 8.0* software.

$$S = S_0 + A e^{(-k/t)} \quad (4)$$

$$S = S_R + (S_i - S_R) e^{-kt} \quad (5)$$

In this expression, S is the substrate concentration (mg·L⁻¹); S_0 is the initial substrate concentration (mg·L⁻¹); S_R is the residual substrate concentration (mg·L⁻¹); t is

time (d); and k is the decay rate constant (d^{-1}). From the k results obtained in the kinetic modelling, the instantaneous substrate consumption rates (r_s) were calculated using Equation (6):

$$r_s = -k \cdot S_o \quad (6)$$

Harvest

Biomass was harvested by flocculation, using a 2.0 L decanter. Flocculation was carried out with wastewater at the outlet of the bubble column photobioreactors (PBRs), adding $2.0 \text{ mL} \cdot \text{L}^{-1}$ of the aluminium sulphate flocculant solution (0.16 M) for decanting the biomass. After about 30 minutes at rest, the phases separated with the concomitant decantation of the biomass in the lower phase of the beaker.

After separating the phases, excess water was removed from the surface, and then, the decanted biomass was filtered using a filtration system composed of a Kitasato flask and a Büchner funnel with qualitative filter paper (Unifil ETQ – 185 mm).

The wet biomass was uniformly distributed over a watch glass and taken to dry in an oven at a temperature of 55–60 °C for a period of 24 hours and subsequently placed in desiccators in order to stabilize the mass at room temperature (Zorn *et al.* 2017). After reaching constant mass, the biomass was crushed using a porcelain and pistil gral until it reached a homogeneous powder.

Lipids extraction

The method used in the extraction of lipids via organic solvents was developed following the methodology by Zorn *et al.* (2017). This methodology promotes a higher lipid yield during the extraction process and is characterized by the use of microalgal biomass with 64% humidity, a chloroform:methanol:water ratio of 5.7:3:1, a total of 33 mL of solvents, and only 70 minutes of ultrasound.

Biomass and lipid productivity

The biomass concentration was quantified by spectrophotometry and the lipid content by extraction with organic solvents. These values were leveraged for calculation of

the biomass productivity (P_B) through Equation (7) and the lipid productivity (P_L) through Equation (8). The calculation of the lipid productivity was performed by multiplying the biomass productivity (P_B) by the mass fraction of lipids (F_M). The calculation of the mass fraction of lipids (F_M) was done using Equation (9):

$$P_B = \frac{(X_F - X_O)}{(t_F - t_O)} \quad (7)$$

$$P_L = P_B * F_M \quad (8)$$

$$F_M = \frac{L_E}{X_E} \quad (9)$$

In these expressions, P_B is the biomass productivity ($\text{g} \cdot \text{L}^{-1} \cdot \text{d}^{-1}$); P_L is the lipids productivity ($\text{g} \cdot \text{L}^{-1} \cdot \text{d}^{-1}$); X_F is the final concentration of biomass ($\text{g} \cdot \text{L}^{-1}$); X_O is the initial concentration of biomass ($\text{g} \cdot \text{L}^{-1}$); F_M is the mass fraction of lipids present in the biomass (%); L_E is the mass of lipids extracted (g); X_E is the amount of biomass used in the extraction (g); and t is the time (d).

Statistical analysis

To statistically confirm which conditions had the greatest influence on the biomass production process (response variable), ANOVA (analysis of variance) was used. The ANOVA was performed using *Minitab* software version 17 and a 95% confidence interval (p -value = 0.05). The biomass productivity (P_B) data, used in the statistical analysis, were calculated (Equation (7)) from the biomass concentration results obtained by spectrophotometry during the monitoring of the cultures in the bubble column photobioreactors (PBRs).

RESULTS AND DISCUSSION

Microbial growth kinetics

The biomass production results obtained in each condition of the kinetic assay were adjusted to the modified Gompertz model to obtain the maximum specific growth rates (μ_{\max}). Each condition tested (C_1 , C_2 , C_3 , C_4 , C_5 , and C_6) has

different concentrations of ammoniacal nitrogen (N-NH_x), as described in the section above on 'Microbial growth kinetics assays'. Considering that cell death occurred in condition C₆, the experimental data for microbial growth were not obtained, and therefore, no adjustment was made. The non-linear adjustments performed for each condition of the kinetic assay are shown in Figure 2.

Table 2 was then created for better visualization of the maximum specific growth rate (μ_{\max}) and latency phase duration time (λ) results, obtained from Equation (1) and presented in the section above on 'Kinetic modelling of microbial growth'. The analysis of the errors of the kinetic parameters was performed using Standard Error (SE) and the Adjusted R-Square (R^2), while the analysis of the errors of the initial concentrations of ammoniacal nitrogen (N-NH_x) was performed using the Standard Deviation (SD).

Despite the absence of ammoniacal nitrogen (N-NH_x) in the control experiment, there was cell growth in this condition because the nitrogen source was present in the form of nitrate (N-NO_3^-), due to supplementation with Bold's Basal Medium (BBM). By interpreting the data, it is possible to observe that the increase of substrate concentration (N-NH_x) in the culture medium provided an increase in the maximum specific growth rates (μ_{\max}). However, conditions with ammoniacal nitrogen concentrations higher

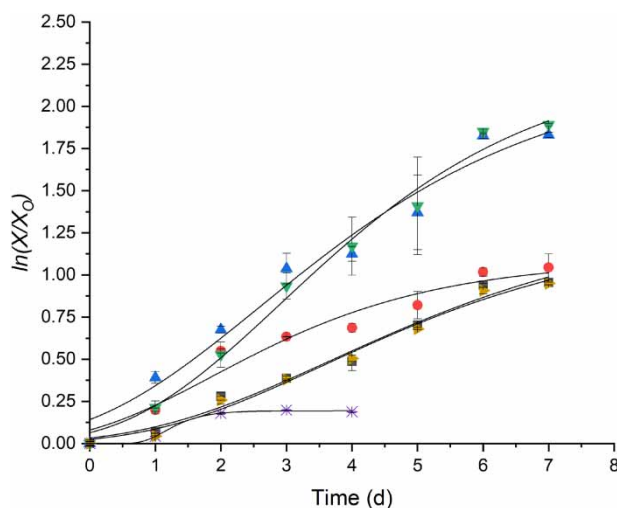


Figure 2 | Growth of *Chlorella vulgaris* microalgae under different concentrations of ammoniacal nitrogen (N-NH_x): Condition 1 (■); Condition 2 (●); Condition 3 (▲); Condition 4 (▼); Condition 5 (*); Control (◆); modified Gompertz model (—).

Table 2 | Kinetic parameters obtained through non-linear adjustments (modified Gompertz kinetic model) and initial ammoniacal nitrogen concentration (N-NH_x) of each condition

Condition	N-NH_x ($\text{mgN-NH}_4^+\cdot\text{L}^{-1}$)	μ_{\max} (d^{-1})	λ (d)	R^2
Control	0.00 ± 0.00	0.179 ± 0.026	0.97 ± 0.27	0.9879
C ₁	7.05 ± 0.08	0.177 ± 0.018	0.89 ± 0.31	0.9832
C ₂	14.09 ± 0.16	0.240 ± 0.055	0.10 ± 0.43	0.9716
C ₃	28.19 ± 0.31	0.316 ± 0.047	0.03 ± 0.42	0.9733
C ₄	56.38 ± 0.62	0.363 ± 0.035	0.63 ± 0.24	0.9904
C ₅	112.76 ± 1.24	0.211 ± 0.029	0.80 ± 0.04	0.9986
C ₆	169.14 ± 1.87	0.000 ± 0.000	0.00 ± 0.00	0.0000

than $56.8 \text{ mgN-NH}_4^+\cdot\text{L}^{-1}$ presented a decrease in the maximum specific growth rate (μ_{\max}), indicating inhibition due to excess substrate (Azov & Goldman 1982).

Analyzing the results of the latency phase duration time (λ), it can be observed that the time was relatively low under all conditions, proving that the inoculum adaptation process to the wastewater was efficient. It is noted that the control showed the largest latency phase among the tested conditions and that as the availability of ammoniacal nitrogen in the medium increased, the latency phase (λ) was reduced. This is likely due to the fact that microalgae have higher affinity to ammoniacal nitrogen compared with oxidized nitrogen compounds, which require a higher energy consumption in the assimilation process (Maestrini et al. 1986). However, conditions C₄ and C₅ presented considerably higher ammoniacal nitrogen concentrations and demonstrated a gradual increase in the latency phase.

Thus, after evaluating the behavior of maximum specific growth rates (μ_{\max}) and latency phase duration time (λ), the Andrews model (Equation (2)) was proposed and adjusted to describe the behavior of microorganisms. From the model, the kinetic parameters μ_{\max} , K_s , and K_i were determined to be 1.27 d^{-1} , $50.25 \text{ mg}\cdot\text{L}^{-1}$, and $28.12 \text{ mg}\cdot\text{L}^{-1}$, respectively. The fit to the Andrews model is illustrated in Figure 3.

Since the Andrews kinetic model adjusted satisfactorily to microbial growth ($R^2 = 0.872$) and there was inhibition by substrate excess, the optimal substrate concentration ($S_{\text{opt}} = 37.59 \text{ mgN-NH}_4^+\cdot\text{L}^{-1}$) was determined (Equation (3)). Tam & Wong (1996) also performed experiments to evaluate the influence of ammoniacal nitrogen concentration on the

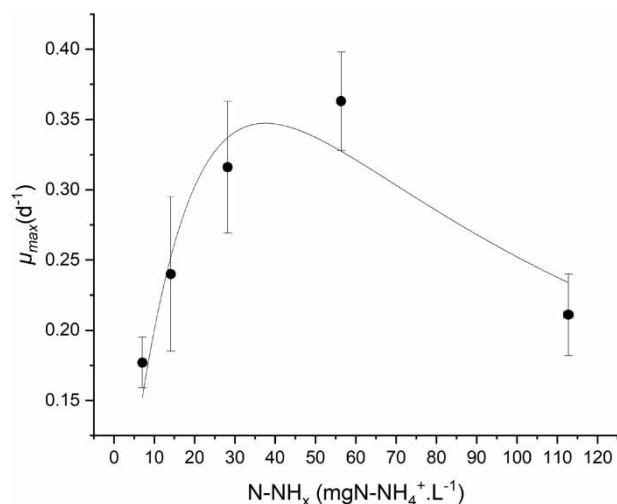


Figure 3 | Maximum specific growth rate (μ_{\max}) of microalgae in relation to the concentration of ammoniacal nitrogen (N-NH_x) present in wastewater (Andrews kinetic model): maximum specific growth rate (●); Andrews model (—).

growth of *C. vulgaris* microalgae. The assays were performed in synthetic culture media with different concentrations of ammoniacal nitrogen (exclusive source of nitrogen in the medium). By contrast, the current study cultivated microalgae photoautotrophically in conical reactor flasks with a useful volume of 400 mL, operated in batch without CO_2 feed and with pneumatic agitation.

Comparing the results of the optimal ammoniacal nitrogen concentrations (S_{opt}), it is possible to observe that the concentration obtained by Tam & Wong (1996) was approximately six times higher. This variation is predictable because in the test by Tam & Wong (1996), pH was 7.0 and ammonium chloride was used as the nitrogen source. Therefore, due to the displacement of the chemical equilibrium of the reaction, all ammoniacal nitrogen was present in the ionic form of ammonium (N-NH_4^+), which is less toxic to microalgae (Li *et al.* 2019). However, in the kinetic test performed in the present work, the pH was adjusted and monitored at 7.5 and industrial wastewater was used as a nitrogen source. Consequently, a portion of the ammoniacal nitrogen (N-NH_x) was present as free ammonia (N-NH_3), which is toxic to the metabolism of microorganisms (Li *et al.* 2019). According to Azov & Goldman (1982), if the culture pH is close to or above 8.0, algal photosynthesis is inhibited by free ammonia concentrations of $28 \text{ mg} \cdot \text{L}^{-1}$. This explains why Tam & Wong (1996) observed that

Chlorella vulgaris still maintained some growth at $1,000 \text{ mg} \cdot \text{L}^{-1}$ ammoniacal nitrogen concentrations and reported an operating S_{opt} that was six times higher.

The pH of the cultures was monitored daily during the kinetic assay, increasing between 0.1 to 0.4 per day. The variations were corrected to the initial value of 7.5 by adding aliquots of sulfuric acid (0.05 M). The constant variation in the pH of the culture medium is explained by the photosynthetic fixation of CO_2 resulting in the shift of pH to alkalinity (Chojnacka & Marquez-Rocha 2004). Previous reports have stated that normally in mixotrophic crops, the final pH of the assays will depend on the dominant, autotrophic or heterotrophic metabolism, and it generally remains constant throughout the processes (Kong *et al.* 2011). Therefore, due to the constant increase in pH, it can be suggested that the predominant metabolism during microalgae growth in the kinetic assay was autotrophic metabolism.

Regarding the maximum specific growth rate (μ_{\max}) values obtained in both the optimal substrate concentrations of this project (0.363 d^{-1}) and the work of Tam & Wong (1996) (0.236 d^{-1}), the significant difference between the results is justified. There was better hydrodynamic behavior of the vials within the shaker (complete mix) compared with the conical flasks with pneumatic agitation, eliminating dead zones, and favoring system homogenization, as well as mass transfer between substrate and microorganisms (Muharam *et al.* 2018).

The dissolved oxygen (DO) of the reactor flasks was also monitored daily during the kinetic test cultures, presenting no changes in relation to their initial concentration ($\text{DO} = 5.69 \text{ mgO}_2 \cdot \text{L}^{-1}$). Thus, it is possible to state that the proposed headspace degassing strategy was efficient.

Cultivation in bubble column photobioreactors (PBRs)

Kinetic modelling of microalgae growth

After obtaining the kinetic parameters for microbial growth (see section 'Microbial growth kinetics') and determining the optimum substrate concentration for operation, the column bubble photobioreactors (PBRs) were started in batch. The microbial growth curves were fitted to the modified Gompertz kinetic model by the Origin 8.0 software. Adjustments to the growth of microalgae in bubble column

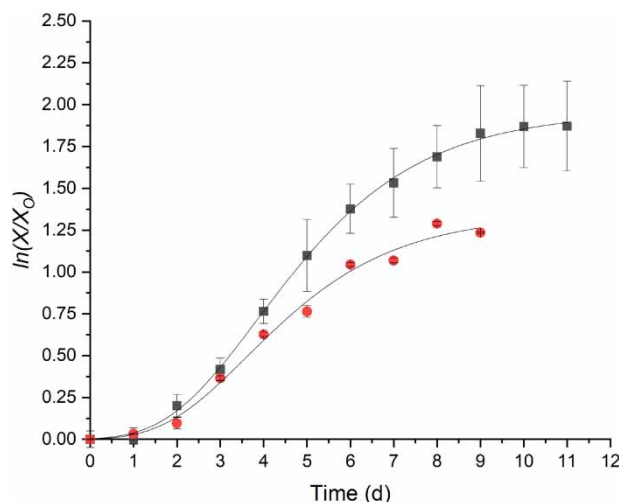


Figure 4 | Growth of *Chlorella vulgaris* microalgae in bubble column photobioreactors (PBRs) fed with wastewater and with Bold's Basal Medium (control): wastewater (■); control (●); modified Gompertz model (—).

photobioreactors (PBRs) fed with wastewater and with Bold's Basal Medium (control) are illustrated in Figure 4.

From the nonlinear adjustments of the kinetic models, the maximum specific growth rates (μ_{\max}) and the duration of the latency phase (λ), obtained in the preparation of Table 3, were obtained for better visualization and interpretation of the results. In addition to the kinetic parameters obtained during kinetic modelling, the biomass productivity (P_B) of the photobioreactors was also calculated and is presented in Table 3. The analysis of the errors of the kinetic parameters was performed using Standard Error (SE) and the Adjusted R-Square (R^2), while the analysis of the errors of biomass productivity (P_B) was performed using the Standard Deviation (SD).

It can be observed that the maximum specific growth rates (μ_{\max}) of the cultures in the photobioreactors, operated under the optimal conditions determined by the kinetic test of microbial growth, reached values very close (0.34 d^{-1}) to those obtained in condition C_4 of the kinetic test (0.36 d^{-1}). Therefore, it is possible to state that the mathematical

modelling of the process (section 'Microbial growth kinetics') was coherent and provided an optimized operation of the PBRs, corroborating the result of Eze et al. (2018).

Analyzing the results presented in Tables 3 and 2, it is possible to observe that there was a longer duration of the latency phase (λ) in the cultures grown in the bubble column photobioreactors (PBRs). This increase in the duration of the latency phase (λ) is justified by the fact that the pneumatic agitation system of the bubble column photobioreactors was not as efficient as the shaker in the homogenization and mass transfer processes. Thus, it is noted that the bubble-column-type photobioreactors did not operate as ideal batch mix reactors, resulting in a longer adaptation period for the microorganisms, corroborating the result of López-Rosales et al. (2019) and Muharam et al. (2018).

Comparing the results of μ_{\max} and X_F obtained, it is possible to verify that in the microalgae cultivations in bubble column photobioreactors (PBRs), the addition of ammoniacal nitrogen (N-NH_x) provided an increase in both the maximum specific growth rate (0.34 d^{-1}) and the production of biomass ($1.83 \text{ g} \cdot \text{L}^{-1}$) with respect to the negative control. This is attributed to the greater affinity of microorganisms to nitrogen in reduced forms (N-NH_x), which lessens the energy expended to reduce and assimilate oxidized nitrogen compounds (N-NO_2^- and N-NO_3^-). Therefore, although it is necessary to dilute the effluent, the increase in the maximum specific growth rates (μ_{\max}) and the production of biomass (X_F) demonstrate the potential of cultivating *C. vulgaris* in anaerobically digested wastewater from food industries.

Mansouri (2017) modelled the growth of photoautotrophically grown *C. vulgaris* microalgae in 20 L airlift photobioreactors, and they used an artificial culture medium (BG-11) with only nitrate ($1.5 \text{ g} \cdot \text{L}^{-1}$) as a nitrogen source. In this work, the kinetic model that provided the best fit was the Baranyi model ($R^2 = 0.989$); however, the

Table 3 | Biomass productivity and kinetic parameters obtained through non-linear adjustments (modified Gompertz model) in the growth of microalgae in bubble column photobioreactors (PBRs)

Condition	$\text{N-NH}_x \text{ (mgN-NH}_4 \cdot \text{L}^{-1})$	$P_B \text{ (g} \cdot \text{L}^{-1} \cdot \text{d}^{-1})$	$\mu_{\max} \text{ (d}^{-1})$	$\lambda \text{ (d)}$	R^2
Control	0.0 ± 0.00	0.081 ± 0.005	0.256 ± 0.024	1.68 ± 0.23	0.992
PBRs with wastewater	44.30 ± 3.47	0.141 ± 0.021	0.343 ± 0.009	1.77 ± 0.08	0.999

modified Gompertz model also showed a good Adjusted R-Square ($R^2 = 0.954$). In adjusting to the Baranyi model, Mansouri (2017) obtained a maximum specific growth rate (μ_{\max}) of 0.741 d^{-1} and biomass production (X_F) of $1.81 \text{ g} \cdot \text{L}^{-1}$. The value of μ_{\max} reported by Mansouri (2017) was higher than that obtained in the present study, while the production of biomass (X_F) reached nearly equal values. The difference in the maximum specific growth rates (μ_{\max}) is justified because the cultures were performed in two different photobioreactor configurations (bubble column and airlift) and used a high concentration of nitrate ($1.5 \text{ g} \cdot \text{L}^{-1}$). Airlift photobioreactors provide a more uniform and efficient distribution of air bubbles in the system because of the internal tube installed in this reactor type, which reduces the bubble sizes and directs the gas flow. Consequently, this favors the mass transfer between microorganisms and substrate, as well as the assimilation of carbon dioxide, and thus, a higher maximum specific growth rate can be achieved (Wang *et al.* 2012).

Statistical analysis of biomass productivity

The cell growth results, obtained by spectrophotometry during operation of the bubble column photobioreactors (PBRs), allowed for calculation of biomass productivities (P_B) with Equation (7). With these values (Table 3), analysis of variance (ANOVA) was performed using the *Minitab 17* software, considering a confidence interval of 95% (p -value = 0.05).

Interpreting the ANOVA table, it can be seen that the p -value (0.014) was lower than the confidence interval, that is, there was a statistically significant difference between the biomass productivity averages for the bubble column photobioreactors (PBRs). This confirms the hypothesis that the addition of anaerobically digested wastewater from the food industry results in higher biomass productivity, and the increase in biomass productivity using wastewater was 57.45%.

Kinetic modelling of nitrogen consumption

During the operation of the bubble column photobioreactors (PBRs) fed with wastewater, the concentrations of ammoniacal nitrogen (N-NH_x) were quantified. The results of ammoniacal nitrogen consumption, shown in Figure 5, were

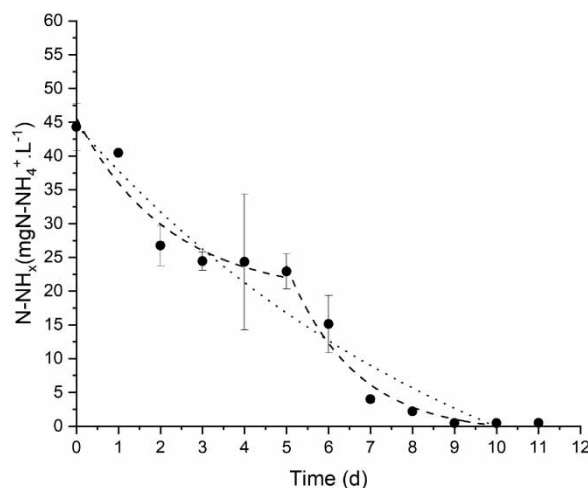


Figure 5 | Adjustment of ammoniacal nitrogen (N-NH_x) consumption in bubble column photobioreactors (PBRs). Subtitle: Experimental data (●); first-order kinetic expression (....); modified first-order kinetic expression (- - -).

adjusted to the first-order kinetic expressions (Equation (4)) and as two decay phases were observed during the consumption of ammoniacal nitrogen, two modified first-order kinetic expressions (Equation (5)) in series were also adjusted.

The first decay phase was from day 1 to day 5, where microalgae still assimilated nitrate, and the second phase of decay was from day 5 to 10, where preference was given to nitrogen in the reduced form (N-NH_x). The second phase demonstrated the interruption of nitrate assimilation, coincidentally resulting in lack of adjustment of the model during this period. The preference for ammoniacal nitrogen began at day 5 due to the greater availability of nitrate in the medium as compared with ammoniacal nitrogen in the beginning of the batch, which favored the mass transfer between substrate and microorganism. Thus, two modified first-order kinetic expression adjustments were proposed for the phases of N-NH_x consumption, named as Phase 1 and Phase 2 (before and after the interruption of nitrate assimilation), respectively. Based on the kinetic parameters obtained, Table 4 is provided to better visualize these results. The analysis of the errors of the kinetic parameters was performed using Standard Error (SE) and the Adjusted R-Square (R^2).

Analyzing the Adjusted R-Square (R^2), it is possible to verify that the modified first-order kinetic expression adjusted satisfactorily to the two phases of substrate consumption in the bubble column photobioreactors (PBRs).

Table 4 | Kinetic parameters of ammoniacal nitrogen consumption (N-NH_4)

Kinetic model	Phase	k (d^{-1})	r_s ($\text{mg}\cdot\text{L}^{-1}\cdot\text{d}^{-1}$)	R^2
First-order kinetic expression	Single phase	0.100 ± 0.052	4.430 ± 2.302	0.9375
Modified first-order kinetic expression	Phase 1	0.453 ± 0.283	20.058 ± 12.531	0.8637
Modified first-order kinetic expression	Phase 2	0.616 ± 0.156	14.219 ± 3.601	0.9529

Although the adjustment to single phase achieved a good Adjusted R-Square (R^2), the analysis of substrate consumption by parts proved to be more adequate to explain the consumption of nitrogen forms present in the bulk liquid. Regarding the ammoniacal nitrogen decay rate constants (k), it was observed that from the fifth day on when the nitrate consumption was interrupted (Figure 6), the microalgae channelled all their energy into the assimilation of ammoniacal nitrogen, and consequently, there was an increase in the decay rate constant from 0.453 to 0.616 d^{-1} . However, the initial substrate concentration (C_0) was lower in phase 2, and although the k values increased, the instantaneous substrate consumption rates (r_s) decreased. It is important to note, however, that both r_s results were considerably superior to those obtained by Choi & Lee (2013) in their study.

Interpreting the behavior of the substrate decay and cell growth curves shown in Figure 6, it is possible to observe that during the first five days, the microalgae consumed nitrate and ammoniacal nitrogen. During the period between days 3 and 5, the consumption of both ammoniacal

nitrogen and nitrate was impaired. After the fifth day, the consumption of nitrate completely ceased, while ammoniacal nitrogen was assimilated until the stationary phase of growth of the microorganisms. This behavior confirms the results obtained by Scherholz & Curtis (2013), who cultivated photoautotrophic cultures of *Chlorella vulgaris* and *Chlamydomonas reinhardtii* in 1.5 L photobioreactors containing substrate concentrations of $0.0135 \text{ gN-NH}_4^+\cdot\text{L}^{-1}$ with chloride and nitrate as ions (NH_4Cl and NH_4NO_3). In this study, when ammoniacal nitrogen and nitrate were supplied simultaneously, the microalgae *Chlorella vulgaris* and *Chlamydomonas reinhardtii* gave preference to the consumption of ammoniacal nitrogen, inhibiting the consumption of nitrate. However, the observation of Li et al. (2019) that microalgae will first consume ammoniacal nitrogen, then nitrite, and finally nitrate could not be verified.

Florencio & Vega (1983) monitored the concentrations of ammoniacal nitrogen and nitrate during the growth of microalgae, since ammoniacal nitrogen also inhibited the use of nitrate and nitrite. Tischner & Lorenzen (1979) stated that depending on the amount of ammoniacal nitrogen added to the medium, this inhibition can last for a long period until the initial rate of nitrate uptake is reached again. This series of results confirms the suspicion about ammoniacal nitrogen uptake and reduction of nitrate expressed by Pistorius et al. (1978).

Total lipid content and lipid productivity

After harvesting the biomass, the total lipid content was determined, and the lipid productivity of the bubble column photobioreactors (PBRs) was calculated. The total lipid content was 0.1245 grams, representing a mass fraction of 12.45%, while the lipid productivity was $17.63 \text{ mg}\cdot\text{L}^{-1}\cdot\text{d}^{-1}$. The mass fraction of accumulated lipids

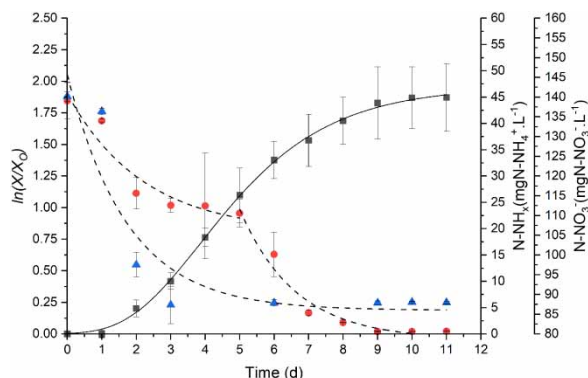


Figure 6 | Biomass growth and substrate consumption in bubble column photobioreactors (PBRs) fed with wastewater: growth experimental data (●); ammoniacal nitrogen experimental data (●); nitrate experimental data (▲); modified Gompertz model (—); modified first-order kinetic expression (---).

obtained in the present work can be compared with the results presented by [Safi *et al.* \(2014\)](#), who considered that microalgae of the species *C. vulgaris* accumulate between 5.0% and 58.0% of lipids. Thus, it can be determined that the mass fraction obtained (12.45%) in the current study was relatively low. This fact is justified by the theory described by [Tan & Lee \(2016\)](#), who stated that the concentration of accumulated lipids is inversely proportional to the availability of nitrogen in the culture medium. Therefore, as the concentration of total nitrogen present in the medium was extremely high during and also after the growth period, the content of total lipids accumulated by the microalgae was low. Thus, the results suggest that microalgae grown under ideal conditions produce large amounts of biomass and present low neutral lipid content, while microalgae grown with a shortage of nutrients accumulate high levels of neutral lipids and grow slowly.

[Matos *et al.* \(2015\)](#) cultivated microalgae of the species *Chlorella* sp. in 4.0 L inverted conical bioreactors, operated in batch, with constant aeration, and at a temperature of 27 °C. The bioreactors were fed with artificial culture medium (BBM) and a desalination concentrate. The basal medium had a concentration of 250 mg·L⁻¹ of nitrate, while the desalination concentrate had 1.35 mg·L⁻¹ of ammonium and 30 mg·L⁻¹ of total nitrogen. In this study, a maximum total lipid percentage of 11.46% and maximum lipid productivity of 19.6 mg·L⁻¹·d⁻¹ were achieved, and these values are similar to those obtained in the present project.

[Guimarães *et al.* \(2019\)](#) cultivated microalgae *Chlorella vulgaris* in 5.0 L bubble column photobioreactors under constant lighting and aeration. The photobioreactors (PBRs) were fed with domestic effluent collected from the aerobic biological reactor in the effluent treatment station at the Lorena Engineering School at the University of São Paulo. The wastewater had a concentration of 10.88 mg of N-NO₃⁻. In this study, the accumulated lipid content was 16.4%, and the lipid productivity was 0.0126 g·L⁻¹·d⁻¹. The lipid content was higher than that obtained in the present project due to the low availability of nitrogen in the domestic effluent; however, the lipid productivity was lower because although the lipid content percentage was high, the biomass productivity was low (0.0552 g·L⁻¹·d⁻¹). This phenomenon is explained by the fact that the availability of substrate is a limiting step in the balance of

growth and production of fatty acids, and thus, the biomass and fatty acid synthesis pathways compete for the same substrates ([Tan & Lee 2016](#)).

In the study by [Guimarães *et al.* \(2019\)](#), biomass production ended, and the nutrient availability was reduced while the photobioreactors were kept in operation for a few more days in order to promote the stress of microorganisms. The difference from the present project is notable, as the batch was interrupted at the exact moment when the microorganisms reached the stationary growth phase. Even after the stagnation of biomass production, there was approximately 80 mg·L⁻¹ of nitrate, which prevented the microorganisms from being exposed to critical conditions of low substrate availability in the culture environment.

CONCLUSION

The cultivation of microalgae *C. vulgaris* in bubble column photobioreactors (PBRs) fed with wastewater nutrients proved to be a viable and efficient alternative for both biomass production and the removal of nitrogenous compounds from water, especially ammoniacal nitrogen (N-NH_x). The Andrews model satisfactorily fitted the biomass growth data by presenting a high Adjusted R-Square (R^2), correctly describing the microbial kinetics and providing the optimized process operation. It can be observed that the use of anaerobically digested gelatin industry wastewater resulted in higher specific growth rates and higher biomass productivity, however, the accumulated lipid content per gram of biomass was low despite lipid productivity having been reasonable. Future studies can further elaborate on the potential benefits and limitations of using food industry and process wastewaters for simultaneous nutrient recovery and algal biomass production at larger scale and different cultivation system configurations in order to evaluate system viability, economics, and sustainability.

DATA AVAILABILITY STATEMENT

All relevant data are included in the paper or its Supplementary Information.

REFERENCES

- APHA/AWWA/WEF 1998 *Standard Methods for the Examination of Water and Wastewater*, 20th edn. American Public Health Association/American Water Works Association/Water Environment Federation, Washington, DC, USA.
- Azov, Y. & Goldman, J. C. 1982 Free ammonia inhibition of algal photosynthesis in intensive cultures. *Applied and Environmental Microbiology* **43** (4), 735–739.
- Choi, H. J. & Lee, S. M. 2013 Performance of *Chlorella vulgaris* for the removal of ammonia-nitrogen from wastewater. *Environmental Engineering Research* **18** (4), 235–239.
- Chojnacka, K. & Marquez-rocha, F.-J. 2004 Kinetic and stoichiometric relationships of the energy and carbon metabolism in the culture of microalgae. *Biotechnology* **3** (1), 21–34.
- Eze, V. C., Velasquez-Orta, S. B., Hernández-García, A., Monje-Ramírez, I. & Orta-Ledesma, M. T. 2018 Kinetic modelling of microalgae cultivation for wastewater treatment and carbon dioxide sequestration. *Algal Research* **32** (1), 131–141.
- Florencio, F. J. & Vega, J. M. 1983 Utilization of nitrate, nitrite and ammonium by *Chlamydomonas reinhardtii*: photoproduction of ammonium. *Planta* **158** (4), 288–293.
- Guimarães, D. H. P., Marino, V. F., Blanco, G. C., dos Santos, W. R. & de Moraes Gomes Rosa, M. T. 2019 Viability of the uses of effluent for cultivation of *Chlorella vulgaris* in order to integrate the generation of biofuels with the treatment of water. In: *Proceedings of the 4th Brazilian Technology Symposium (BTSym'18): Emerging Trends and Challenges in Technology* (Y. Iano, R. Arthur, O. Saotome, V. V. Estrela & H. J. Loschi, eds), Springer, Cham, Switzerland, pp. 347–360.
- Janosz Rajczyk, M. 1993 Fermentation of food industry wastewater. *Water Research* **27** (7), 1257–1262.
- Kong, W.-B., Song, H., Cao, Y., Yang, H., Hua, S. F. & Xia, C. G. 2011 The characteristics of biomass production, lipid accumulation and chlorophyll biosynthesis of *Chlorella vulgaris* under mixotrophic cultivation. *African Journal of Biotechnology* **10** (55), 11620–11630.
- Li, X., Li, W., Zhai, J., Wei, H. & Wang, Q. 2019 Effect of ammonium nitrogen on microalgal growth, biochemical composition and photosynthetic performance in mixotrophic cultivation. *Bioresource Technology* **273**, 368–376.
- López-Rosales, L., Sánchez-Mirón, A., Contreras-Gómez, A., García-Camacho, F., Battaglia, F., Zhao, L. & Molina-Grima, E. 2019 Characterization of bubble column photobioreactors for shear-sensitive microalgae culture. *Bioresource Technology* **275**, 1–9.
- Maestrini, S. Y., Robert, J.-M., Leftley, J. W. & Collos, Y. 1986 Ammonium thresholds for simultaneous uptake of ammonium and nitrate by oyster-pond algae. *Journal of Experimental Marine Biology and Ecology* **102** (1), 75–98.
- Mai, D. T., Kunacheva, C. & Stuckey, D. C. 2018 A review of posttreatment technologies for anaerobic effluents for discharge and recycling of wastewater. *Critical Reviews in Environmental Science and Technology* **48** (2), 167–209.
- Mansouri, M. 2017 Predictive modeling of biomass production by *Chlorella vulgaris* in a draft-tube airlift photobioreactor. *Advances in Environmental Technology* **2** (3), 119–126.
- Matos, Â. P., Morioka, L. R. I., Sant'Anna, E. S. & França, K. B. 2015 Teores de proteínas e lipídeos de *Chlorella* sp. cultivada em concentrado de dessalinização residual (Protein and lipid contents of *Chlorella* sp. grown in residual desalination concentrate). *Ciência Rural* **45** (2), 364–370.
- Muharam, Y., Ismail, D. & Wirya, A. 2018 Process optimization of microalgae cultivation in a bubble-column photobioreactor. *IOP Conference Series: Earth and Environmental Science* **105**, 012002.
- Pistorius, E. K., Funkhouser, E. A. & Voss, H. 1978 Effect of ammonium and ferricyanide on nitrate utilization by *Chlorella vulgaris*. *Planta* **141** (3), 279–282.
- Ramsay, I. R. & Pullammanappallil, P. C. 2001 Protein degradation during anaerobic wastewater treatment: derivation of stoichiometry. *Biodegradation* **12** (4), 247–256.
- Safi, C., Zebib, B., Merah, O., Pontalier, P.-Y. & Vaca-Garcia, C. 2014 Morphology, composition, production, processing and applications of *Chlorella vulgaris*: a review. *Renewable and Sustainable Energy Reviews* **35**, 265–278.
- Scherholz, M. L. & Curtis, W. R. 2013 Achieving pH control in microalgal cultures through fed-batch addition of stoichiometrically-balanced growth media. *BMC Biotechnology* **13** (1), 39.
- Tam, N. F. Y. & Wong, Y. S. 1996 Effect of ammonia concentrations on growth of *Chlorella vulgaris* and nitrogen removal from media. *Bioresource Technology* **57** (1), 45–50.
- Tan, K. W. M. & Lee, Y. K. 2016 The dilemma for lipid productivity in green microalgae: importance of substrate provision in improving oil yield without sacrificing growth. *Biotechnology for Biofuels* **9** (1), 255.
- Tischner, R. & Lorenzen, H. 1979 Nitrate uptake and nitrate reduction in synchronous *Chlorella*. *Planta* **146** (3), 287–292.
- Wang, B., Lan, C. Q. & Horsman, M. 2012 Closed photobioreactors for production of microalgal biomasses. *Biotechnology Advances* **30** (4), 904–912.
- Zorn, S. M. F. E., Pedro, G. A., Amaral, M. S., Loures, C. C. A. & Silva, M. B. 2017 Avaliação dos fatores envolvidos na extração de lipídios da biomassa da microalga *Chlorella minutissima* via solventes (Evaluation of the factors involved in the extraction of lipids from the biomass of the microalgae *Chlorella minutissima* via solvents). *Holos* **2**, 66–79.

First received 29 June 2020; accepted in revised form 1 October 2020. Available online 14 October 2020